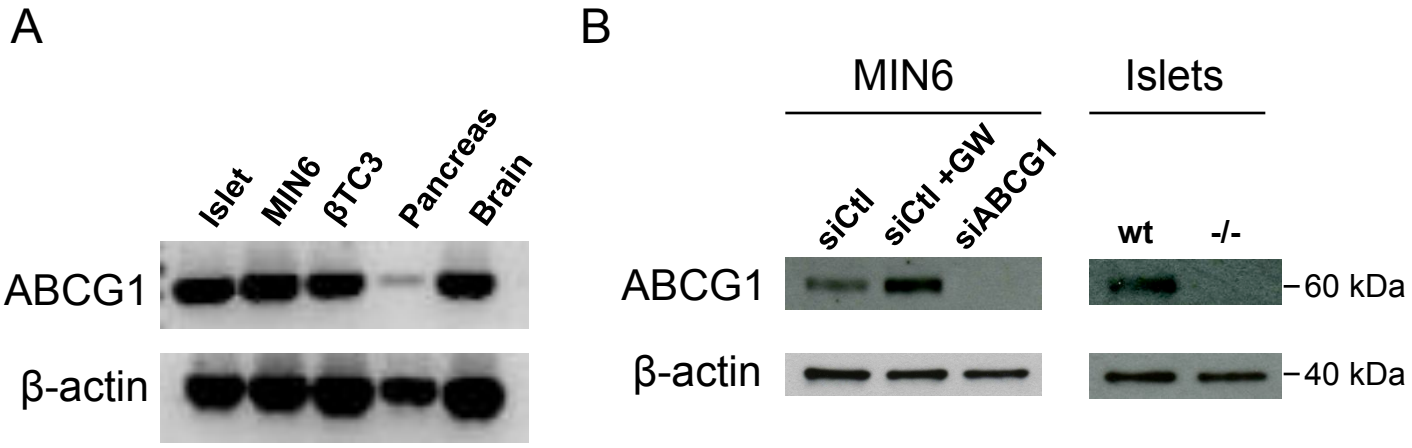

Supplemental Figure 1. ABCG1 is expressed in pancreatic β cells. (A) Conventional PCR was performed for ABCG1 mRNA expression in isolated mouse islets and two mouse β cell lines, MIN6 and βTC3, as well as whole pancreas. Brain is shown as a positive control. (B) MIN6 cells were treated with either an LXR agonist (GW3965) or ABCG1 siRNA and protein was harvested. Western blotting showed presence of ABCG1 protein, and the increase with LXR agonist and decrease with ABCG1 siRNA demonstrated the specificity of the band. Similarly, islets were isolated from WT and *Abcg1*$^{-/-}$ mice and western blotting confirmed presence of ABCG1 protein and the specificity of the band.

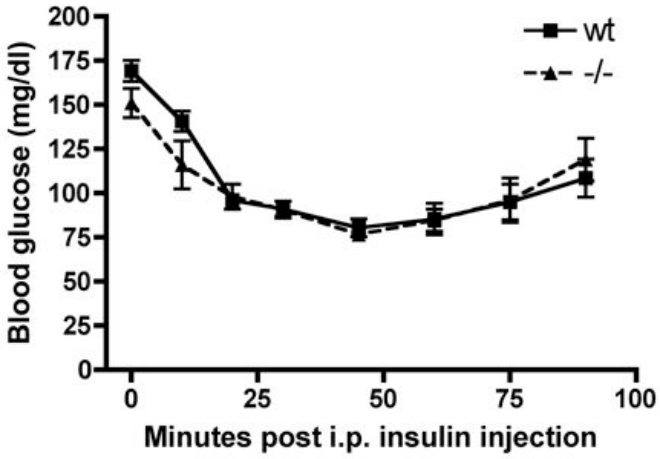

Supplemental Figure 2. *Abcg1*$^{-/-}$ mice have normal insulin tolerance. Male WT and *Abcg1*$^{-/-}$ mice were fasted for 4 hours, insulin was injected i.p., and blood glucose was monitored over 90 minutes (age 3 months, n=6 per genotype).

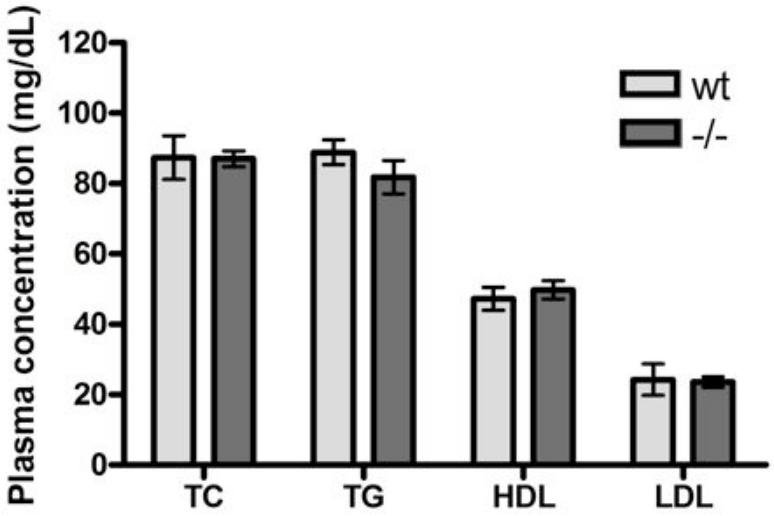

Supplemental Figure 3. *Abcg1*$^{-/-}$ mice have normal plasma lipoprotein profiles. WT and *Abcg1*$^{-/-}$ mice were fasted for 4 hours, plasma was collected, and total-cholesterol (TC), triglycerides (TG), HDL cholesterol, and LDL cholesterol were measured (n=5-8 mice per group).

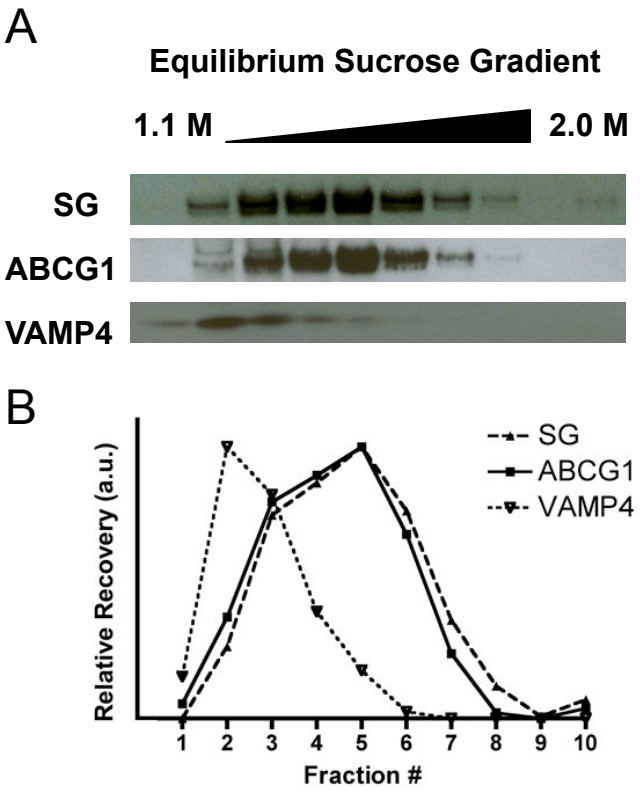

Supplemental Figure 4. Subcellular localization of ABCG1 in adrenal chromaffin-derived PC12 cells. Adrenal-chromaffin derived PC12 cells were homogenized and fractionated as described to isolate secretory granules. Fractions from the equilibrium sucrose gradient were collected and western blotting was performed for ABCG1, the granule marker secretogranin (SG), and the immature granule marker VAMP4.

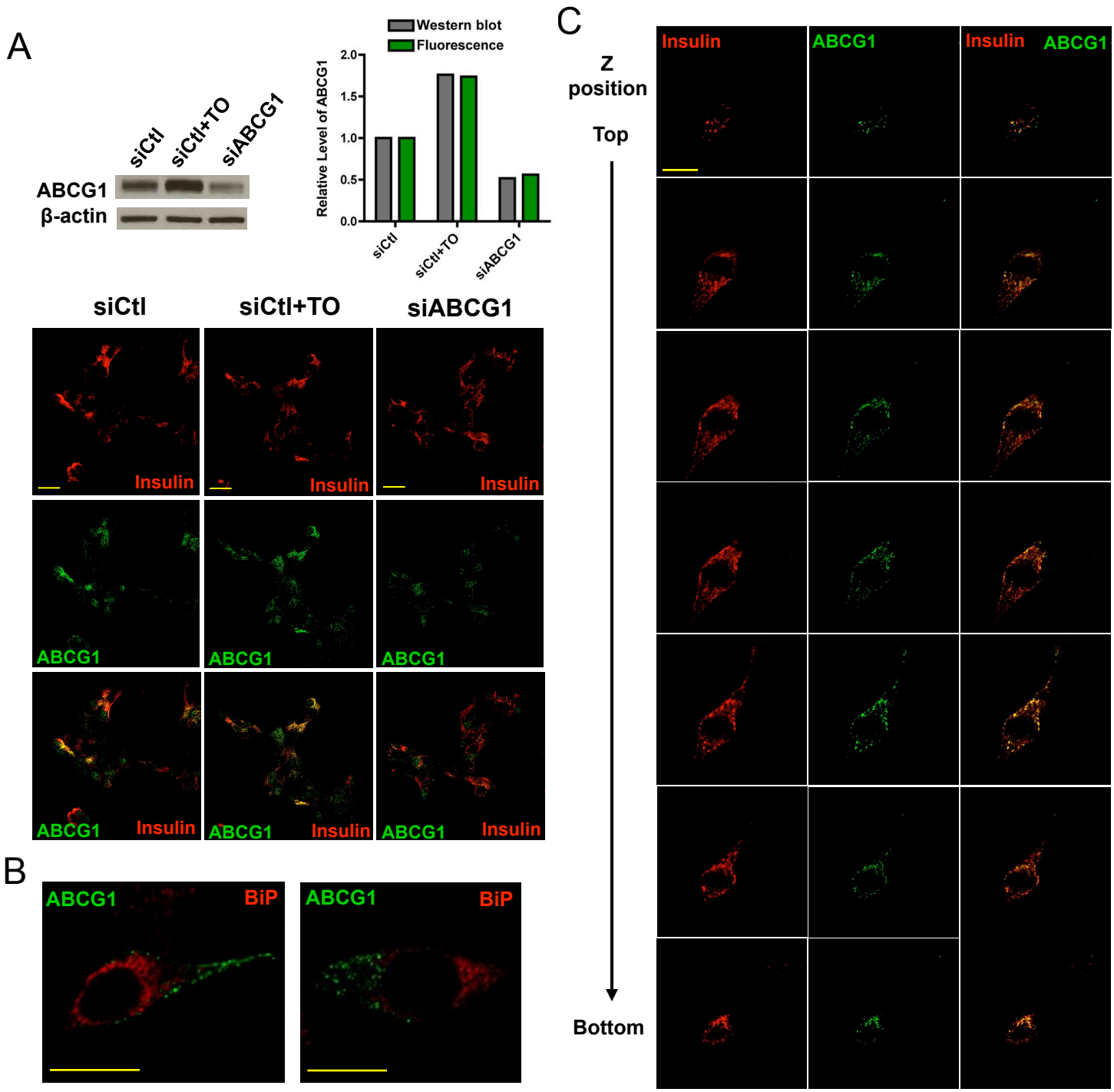

Supplemental Figure 5. Validation of ABCG1 immunofluorescence. MIN6 cells were plated on culture-treated glass slides, fixed, permeablized, and immunostained for ABCG1 (green) and insulin (red). Images were acquired by confocal microscopy. (A) MIN6 cells were treated with control siRNA, control siRNA + 10 μM of LXR agonist (T0901317), or ABCG1 siRNA, then fixed and stained for ABCG1 and insulin. ABCG1 staining localized to discrete, intracellular puncta, and colocalized with insulin. In parallel, protein from identically treated samples was harvested and western blotting was performed. Relative ABCG1 staining was quantified in the western blot, normalized to β-actin; and in immunofluorescence images, normalized to insulin to account for differing cell density across fields. ABCG1 immunofluorescence was induced by TO and reduced by ABCG1 siRNA at levels similar to that quantified by western blot (see graph), indicating that the staining is specific for ABCG1 protein. Note that there is variable background nuclear staining in some cells, but that this was not modified by treatment. (B) MIN6 cells were stained for ABCG1 (green) and another intracellular protein, the ER marker BiP (red); two example images. The lack of colocalization of ABCG1 with BiP demonstrates that ABCG1 does not reside at steady-state in the ER and further supports its specific localization to insulin granules. (C) Images from a confocal Z-stack of ABCG1 and insulin staining in MIN6 cells demonstrating that ABCG1 and insulin colocalize throughout the depth of the sample, and are not merely in adjacent but overlapping organelles. Scale bar = 20 μm(A);10 μm(B,C).

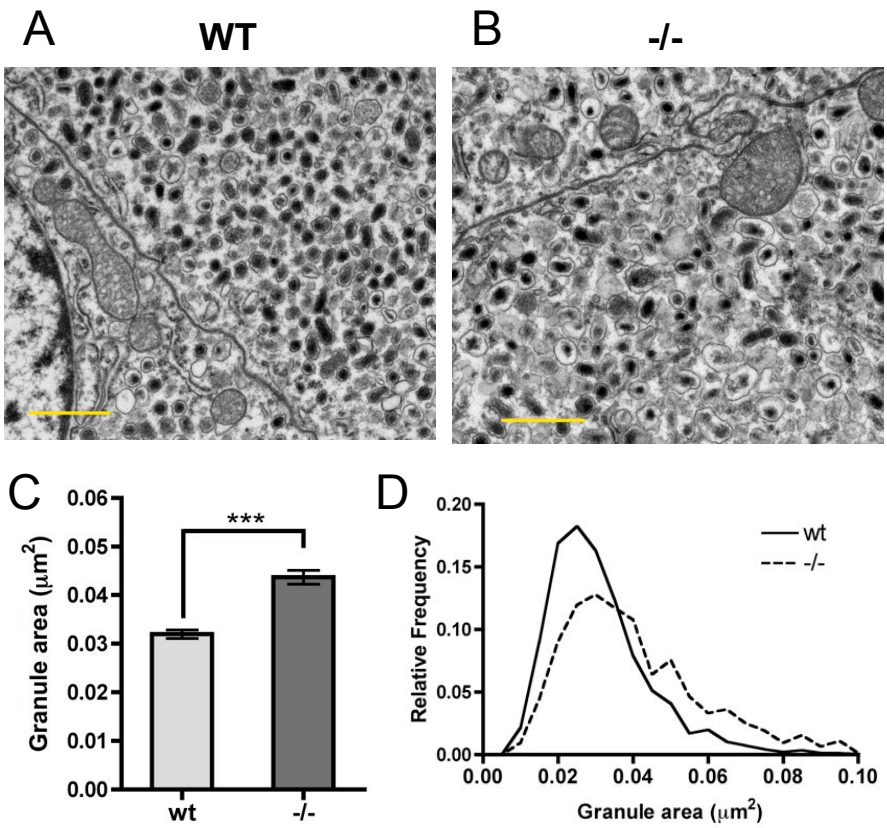

Supplemental Figure 6. Loss of ABCG1 leads to increased membrane-delimited granule area in adrenal chromaffin cells. Adrenal medulla were isolated from WT and *Abcg1*$^{-/-}$ mice and transmission electron microscopy (TEM) was performed to assess granule morphology. (A,B) TEM images from WT and *Abcg1*$^{-/-}$ chromaffin cells. Scale bar = 1 μm. (C,D) Quantification of the granule areas from images as in A and B. (C) Mean granule area ± 95% confidence interval. (D) Relative frequency distribution of granule areas (n granules = 1342(wt), 1353(-/-)).

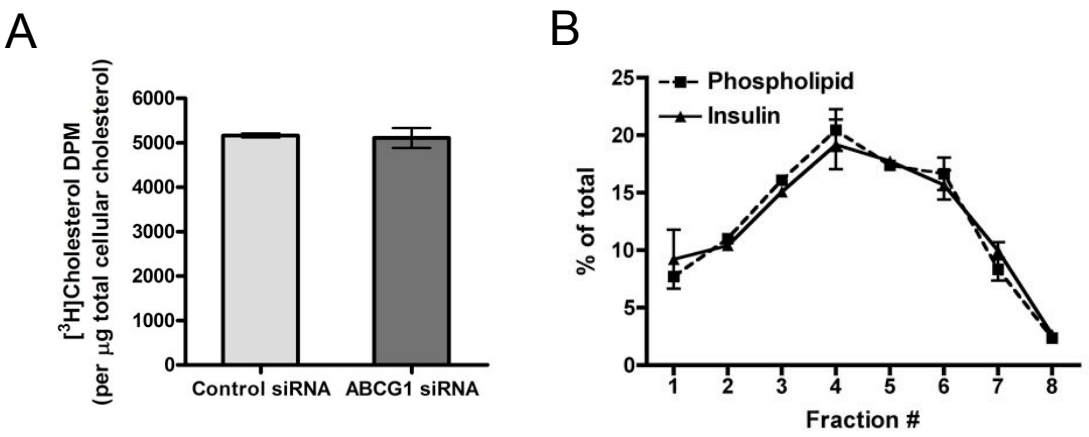

Supplemental Figure 7. Validation of MIN6 granule [^{3}H]cholesterol labeling and fractionation. (A) MIN6 cells were treated with control or ABCG1 siRNA, then 36 hours later were incubated overnight with [^{3}H] cholesterol. Cell lysates were harvested and [^{3}H]cholesterol was normalized to total cellular cholesterol as measured by enzymatic assay (n=3 samples per group). (B) Phospholipid and insulin recoveries were plotted across the iodixanol density gradients from the granule sub-fractionations. Essentially equivalent relative recoveries of insulin and phospholipid across the density gradients indicate that insulin granules contribute the bulk of the membrane lipid in these fractions and that contamination by other organelles is minimal (n=2 gradients). Parent granule fractions were collected on isosmotic iodixanol cushions prior to sub-fractionation to prevent organelle lysis.

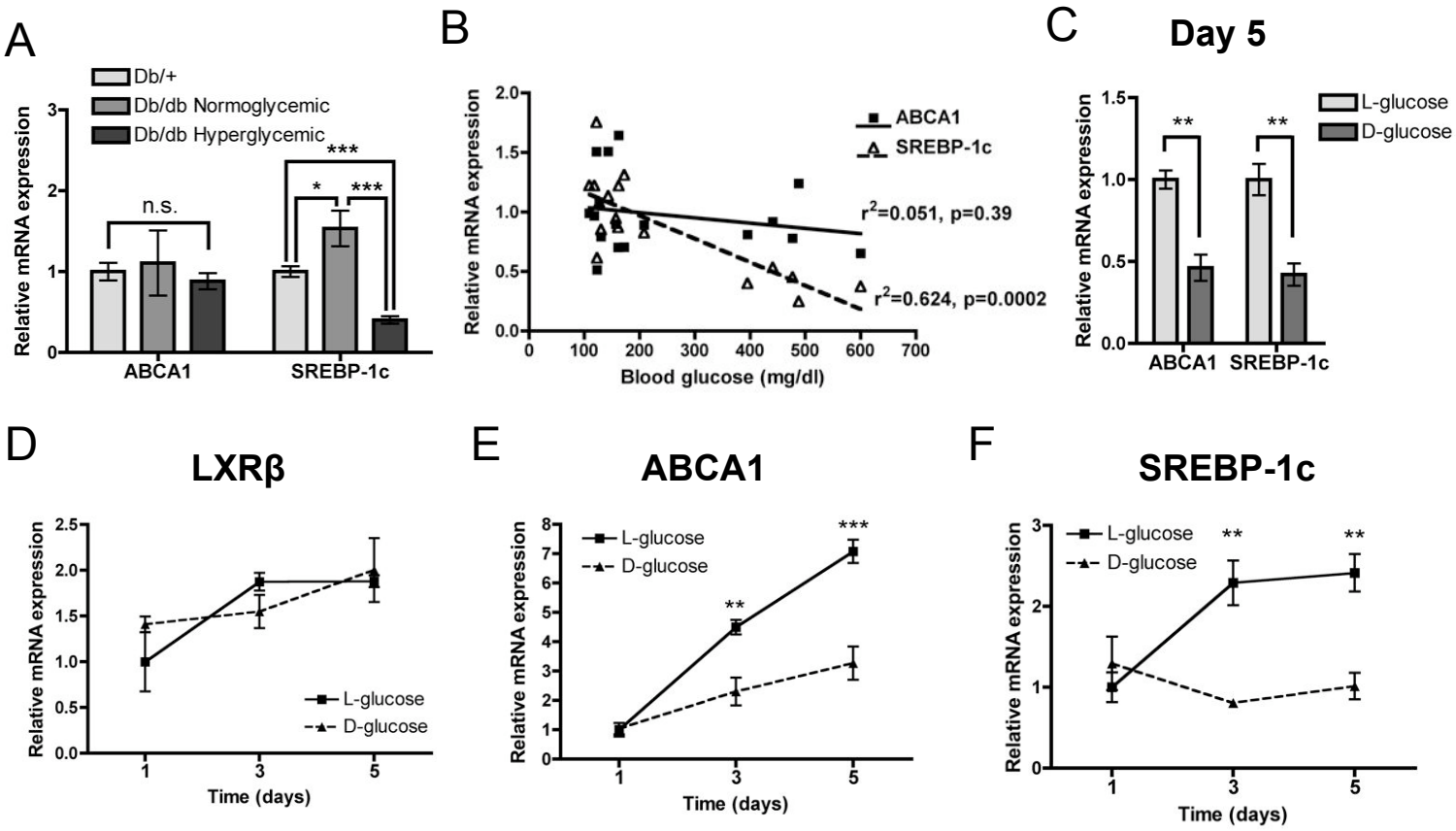

Supplemental Figure 8. Islet expression of the LXR target genes ABCA1 and SREBP-1c in diabetes and in response to high glucose in vitro. (A,B) Islets were isolated from hyperglycemic db/db, normoglycemic db/db, and db/+ control littermates, and mRNA was collected (n=10(db/+);2(db/db normoglycemic);5(db/db hyperglycemic)). (A) qRT-PCR for ABCA1 and SREBP-1c. (B) Linear regression analysis of the correlations between islet mRNA levels of ABCA1 and SREBP-1c, and random blood glucose. (C-F) Isolated mouse islets were cultured for 1, 3, or 5 days in either 25 mM D-glucose or the non-metabolizable L-glucose control (5.5 mM D-glucose + 19.5 mM L-glucose), mRNA was isolated, and qRT-PCR was performed (n=3, representative of 3 independent experiments). (C) Relative expression of ABCA1 and SREBP-1c after 5 days in culture. (D-F) Time-course of expression of (D) LXRβ, (E) ABCA1, and (F) SREBP-1c in response to glucose in culture.